

## Molecular Simulations for Anti-amyloidogenic Effect of Flavonoid Myricetin Exerted against Alzheimer's $\beta$ -Amyloid Fibrils Formation

Youngjin Choi,<sup>†</sup> Thomas Donghyun Kim,<sup>‡</sup> Seung R. Paik,<sup>§</sup> Karpjoo Jeong,<sup>#,\*</sup> and Seunho Jung<sup>¶,\*</sup>

<sup>†</sup>Biochip Research Center, Hoseo University, Asan 336-795, Korea

<sup>‡</sup>Department of Biochemistry, University of Chicago, Chicago, Illinois 60637, U.S.A.

<sup>§</sup>School of Chemical and Biological Engineering, College of Engineering, Seoul National University, Seoul 151-744, Korea

<sup>#</sup>College of Information and Communication & Department of Advanced Technology Fusion, Konkuk University, Seoul 143-701, Korea. \*E-mail: jeongk@konkuk.ac.kr

<sup>¶</sup>Bio/Molecular Informatics Center & Department of Bioscience and Biotechnology, Konkuk University, Seoul 143-701, Korea  
\*E-mail: shjung@konkuk.ac.kr

Received June 27, 2008

Comparative molecular simulations were performed to establish molecular interaction and inhibitory effect of flavonoid myricetin on formation of amyloid fibrils. For computational comparison, the conformational stability of myricetin with amyloid  $\beta$ -peptide ( $A\beta$ ) and  $\beta$ -amyloid fibrils ( $fA\beta$ ) were traced with multiple molecular dynamics simulations (MD) using the CHARMM program from Monte Carlo docked structures. Simulations showed that the inhibition by myricetin involves binding of the flavonoid to  $fA\beta$  rather than  $A\beta$ . Even in MD simulations over 5 ns at 300 K, myricetin/ $fA\beta$  complex remained stable in compact conformation for multiple trajectories. In contrast, myricetin/ $A\beta$  complex mostly turned into the dissociated conformation during the MD simulations at 300 K. These multiple MD simulations provide a theoretical basis for the higher inhibitory effect of myricetin on fibrillogenesis of  $fA\beta$  relative to  $A\beta$ . Significant binding between myricetin and  $fA\beta$  observed from the computational simulations clearly reflects the previous experimental results in which only  $fA\beta$  had bound to the myricetin molecules.

**Key Words :** Amyloid fibril, Conformational analysis, Flavonoid, Molecular dynamics simulations, Myricetin

### Introduction

Amyloidosis is a clinical condition marked by the deposition of fibrous amyloids in various organs and tissues of the body.<sup>1</sup> The protein fibril formation may be causative for various fatal human disorders including Alzheimer's disease (AD).<sup>2</sup> Common structural feature of amyloid fibrils has been characterized by critical cross  $\beta$ -sheet core structure that perpetuates along the fibril long axis.<sup>3</sup> Fibrillogenesis of the monomeric amyloid  $\beta$ -peptide ( $A\beta$ ) found in AD generally occurs *via* nucleation-dependent polymerization.<sup>4</sup> If supersaturated  $A\beta$  solution forms a nucleus, the growth of fibril is accelerated to evolve into the  $\beta$ -amyloid fibrils ( $fA\beta$ ).<sup>5</sup> The structure-toxicity relationship study performed by Riek and co-workers indicates that  $fA\beta$  contain an intrinsic toxicity that correlates with their morphologies as well as quantities.<sup>6</sup> They showed that the neurotoxicity was generally proportional to the size of  $fA\beta$ . Therefore, it would be crucial to regulate the  $fA\beta$  growth by chemical additives to develop potent anti-Alzheimer's disease drugs.

Recent studies for the  $fA\beta$  fibrilization revealed that some flavonoid compounds are able to inhibit the fibril growth and destabilize the preformed  $fA\beta$ .<sup>7</sup> Ono *et al.* found that myricetin exhibited its anti-amyloidogenic effect *via* preferential binding to the  $fA\beta$  rather than the  $A\beta$  monomers.<sup>8</sup> In order to develop anti-amyloidogenic drugs, it is mandatory for structural biologists to acquire a detailed understanding of molecular interactions between flavonoids and

$fA\beta$ .

In this report, comparative molecular simulations were performed for both myricetin/ $A\beta$  and myricetin/ $fA\beta$  in order to explain the experimentally observed inhibitory effect of myricetin for the fibril growth of  $A\beta$ . To reproduce real interactions between myricetin and amyloid peptide, Monte Carlo (MC) docking and molecular dynamics (MD) simulations were carried out for the molecular models of myricetin/ $A\beta$  and myricetin/ $fA\beta$ . Significant binding between myricetin and  $fA\beta$  observed from the computational simulations clearly reflects the previous experimental results<sup>8</sup> in which only  $fA\beta$  bind to the myricetin molecules. From the simulation of fibrillar  $fA\beta$  with myricetin, it has been found that the myricetin interactions with the outermost part of fibrils are responsible for the experimentally observed inhibitory effect on the fibrillogenesis of  $fA\beta$ .

### Results and Discussion

**Differences in docked conformations and energetics of the myricetin with  $A\beta$  and  $fA\beta$ .** The interaction energy profiles of each myricetin complex with  $A\beta$  and  $fA\beta$  during MC docking simulations are shown in Figure 1. The intermolecular energy between myricetin and  $A\beta$  was  $-18.83$  kcal/mol and those of myricetin and  $fA\beta$  was  $-21.41$  kcal/mol during last  $6 \times 10^5$  MC trials. This means that the myricetin molecule forms a more stable complex with  $fA\beta$  than the monomeric  $A\beta$ . This result seems to be consistent

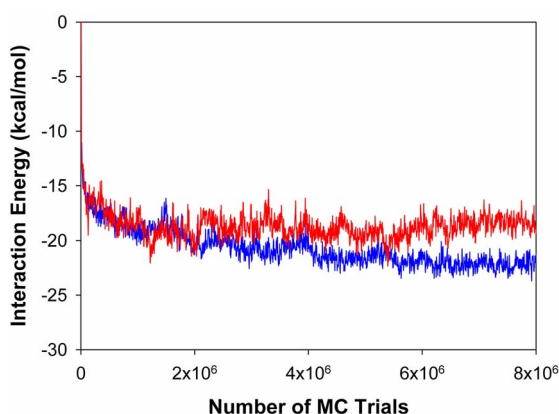


**Figure 1.** Interaction energy profiles of myricetin with helical (red line) or fibrous (blue line) form of amyloid peptide during MC docking simulations.

with the experimental observation that the flavonoid myricetin exerted its binding ability only to  $fA\beta$  rather than  $A\beta$ . Interaction energy profiles of the myricetin/ $A\beta$  and the myricetin/ $fA\beta$  are shown in Figure 2. Myricetin was docked onto a region between  $\alpha$ -helix and C-termini of the  $A\beta$ . There was no special binding site on the  $A\beta$  and the myricetin just clung to the surface of the peptide (Fig. 2). Contrary to the case of myricetin/ $A\beta$ , the myricetin formed a stable docked complex with the  $fA\beta$ . The U-shaped conformation of  $fA\beta$  provided suitable binding site for a flat shaped myricetin molecule.<sup>5</sup> The myricetin was fully stuck into the hydrophobic binding patch of the  $fA\beta$ . These two conformations were further investigated by MD simulations.

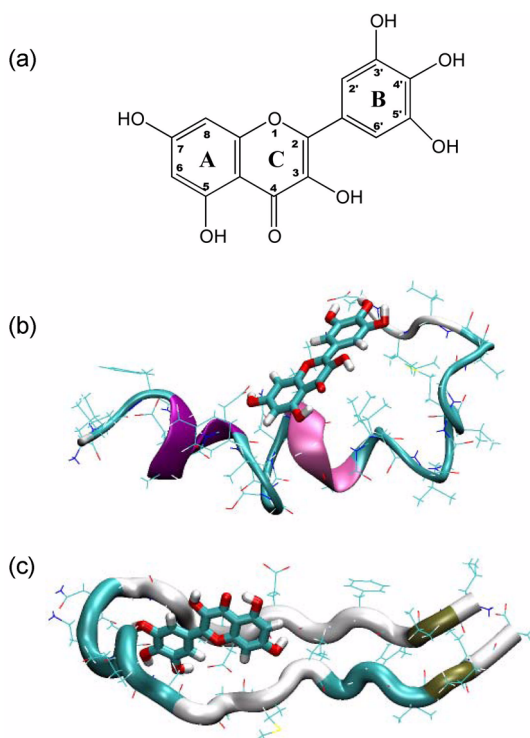


**Figure 2.** The 2-D structure of myricetin (a) and its docked conformation with helical (b) or fibrous (c) form of amyloid peptide.

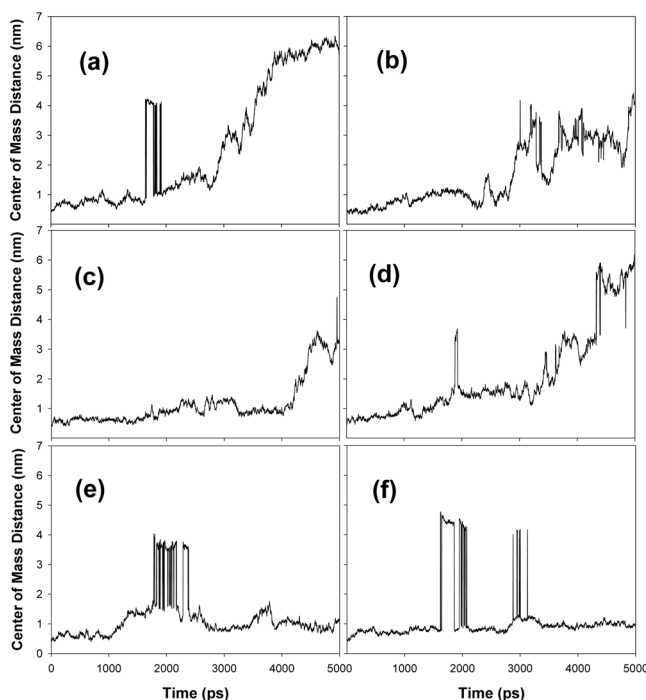


**Figure 3.** Center of mass distances between myricetin and helical form of amyloid during multiple 5ns-MD simulations.

**Complex stability of myricetin/ $A\beta$  and myricetin/ $fA\beta$  during multiple MD simulations.** Multiple MD simulations were performed from the lowest energy conformation of MC simulations. These MD simulations for each myricetin complex evidenced more stable conformation of myricetin/ $fA\beta$  compared to myricetin/ $A\beta$ . Figure 3 shows center of mass distance between myricetin and  $A\beta$  during 5-ns of MD simulations for six trajectories. Four trajectories showed gradual dissociation of the myricetin from  $A\beta$  with some variations (Figure 3a-d). Stable docked conformations were only maintained for just two trajectories with showing high-fluctuations (Figure 3e, f). Therefore, we can conclude that the interaction between myricetin and  $A\beta$  may be weak and unsuitable for keeping the complex stability during MD simulations. Compared with the myricetin/ $A\beta$  complex, the myricetin showed a more stable structure with the  $fA\beta$  during multiple MD simulations. Final dissociation of myricetin from  $fA\beta$  were observed for only two trajectories (Figure 4c, d). Others were tightly associated with each other during MD simulations, in which averaged center of mass distances were 0.83, 0.70, 0.53, and 0.52 nm, respectively (Figure 4a, b, e, f).

The differences in the conformational stability of the myricetin/ $A\beta$  and the myricetin/ $fA\beta$  were also supported by minimum distances between the myricetin and  $A\beta$  or  $fA\beta$  (Figure 5). After 5-ns of MD simulations, trajectory-averaged minimum distance between myricetin and  $A\beta$  was about 3 nm, while the distance between myricetin and  $fA\beta$  was below 2 nm. This means that the atomic interactions between myricetin and  $fA\beta$  were more stable than those of myricetin and  $A\beta$ . Figure 6 is a solvent-accessible surface area change upon formation of complexes between myri-

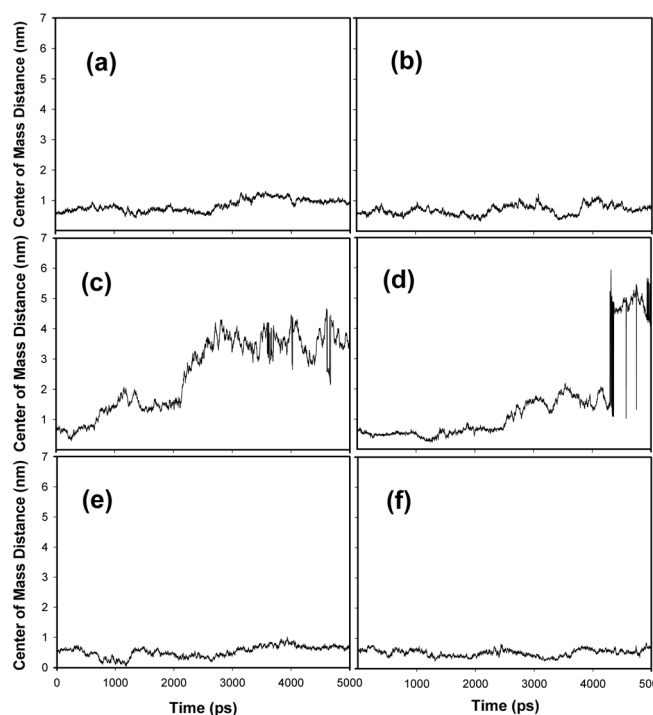


**Figure 4.** Center of mass distances between myricetin and fibrous form of amyloid during multiple 5ns-MD simulations.

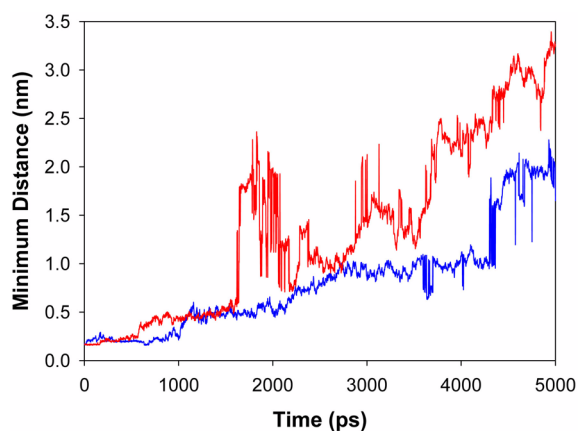


**Figure 5.** Averaged minimum distance between myricetin and helical (red line) or fibrous (blue line) form of amyloid peptide during multiple MD simulations.

myricetin and  $A\beta$  or  $fA\beta$ . At early MD phase (0-1 ns), the surface area change from binding of myricetin to  $fA\beta$  was  $-5.85 \text{ nm}^2$ . This indicates that the surface area was decreased by approximately  $5.85 \text{ nm}^2$  due to the binding of myricetin and  $fA\beta$ . The value was increased to  $-3.70 \text{ nm}^2$  during late MD simulation phase (4-5 ns). For the myricetin/ $A\beta$ , the surface area change was  $-4.40 \text{ nm}^2$  during early MD phase and the value was increased to  $-1.33 \text{ nm}^2$  during late MD phase. The surface area change of myricetin/ $fA\beta$  was much lower than that of myricetin/ $A\beta$  at any MD time phase. These results suggest tighter binding of myricetin to the  $fA\beta$  in comparison to  $A\beta$ . The ratio of surface area changes during late to early MD phase was 0.63 for the myricetin/ $fA\beta$  and 0.30 for the myricetin/ $A\beta$ . This means

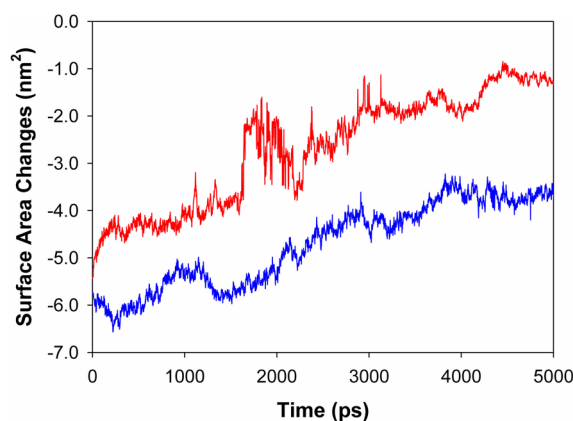


**Figure 6.** Averaged surface area change upon complexation of myricetin with helical (red line) or fibrous (blue line) form of amyloid peptide during multiple MD simulations.

that the surface area decrease of myricetin/ $fA\beta$  was two-fold higher than that of myricetin/ $A\beta$  during the time scale of MD simulations. Therefore, binding stability of myricetin to the  $fA\beta$  is more tolerant to dynamic fluctuation of the molecular complex during the MD simulation time. The strong binding ability of myricetin to  $fA\beta$  in comparison to  $A\beta$  could provide a molecular understanding for experimentally observed inhibitory effect of myricetin on amyloid fibrilligenesis.

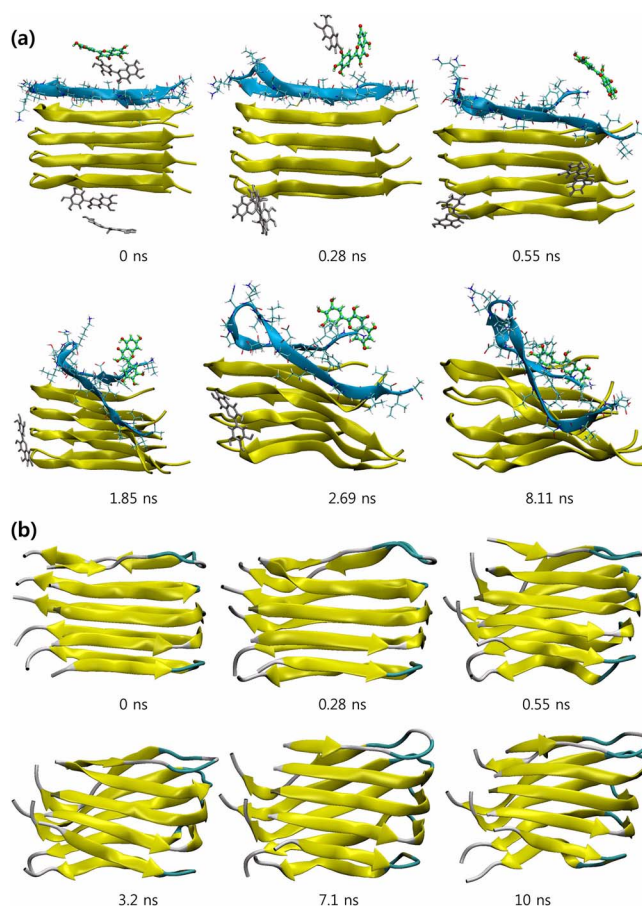


**Figure 7.** Destabilization of  $fA\beta$  fibrils with myricetin (a) and stable  $fA\beta$  fibrils (b) during 10ns MD simulations.

**Destabilization of fA $\beta$  by myricetin during the MD simulations.** Myricetin can destabilize existing fibrils as well as have inhibitory effect on formation of emerging fibrils. Figure 7 is the time course of the fibril destabilization by myricetin during 10-ns of MD simulations. The fibrils were modeled as five sets of fA $\beta$  monomers. After 280 ps, the myricetin made an interaction with the outermost fA $\beta$  sheaf. After 550 ps, the myricetin had bound to C-termini of the fA $\beta$  sheaf *via* hydrophobic interaction of aromatic rings. The binding interaction was intensified into the core cavity of the outermost fA $\beta$  sheaf after 1.85 ns of MD simulation. In that time, about half of the domain of fA $\beta$  sheaf was segregated from remaining fA $\beta$  fibrils. The level of interaction between fibrils and fA $\beta$  part was minimized by the bound myricetin. After 2.69 ns, the myricetin moved out of N-termini of fA $\beta$  sheaf and showed relatively decreased interaction with the fA $\beta$  sheaf. Finally, the myricetin moved to the next part of fA $\beta$  sheaf to destabilize remaining part of fA $\beta$  fibrils after 8.11 ns. From the MD simulation snapshots in the Figure 7, it is evidenced that the myricetin exert an anti-amyloidogenic effect by destabilizing the fA $\beta$  fibrils as well as inhibiting the formation of fibrils from monomeric peptides.

For the quantitative comparison between with and without myricetin conditions, C $\alpha$  atomic distance was analyzed for each fA $\beta$  sheaf in the fibrils. Figure 8 is time course of interatomic distance between fA $\beta$  sheaf 1-2, 2-3, 3-4, and 4-5 for centric C $\alpha$  atom of each Gly13 residue. During the MD simulations, it was found the interatomic distances of outer fA $\beta$  sheaf 1-2 or 4-5 were dramatically increased by myricetin (Figure 8a, d). However the distances for the inner fA $\beta$  sheaf were not changed during the MD simulations for both with and without myricetin conditions (Figure 8b, c). It seems that myricetin molecule exert anti-amyloidogenic effect for outer part of fA $\beta$  fibrils by perturbing these inter-shelf vdw interactions. Figure 9 is intermolecular electrostatic and vdw energy between outermost fA $\beta$  sheaf 1 and 2.

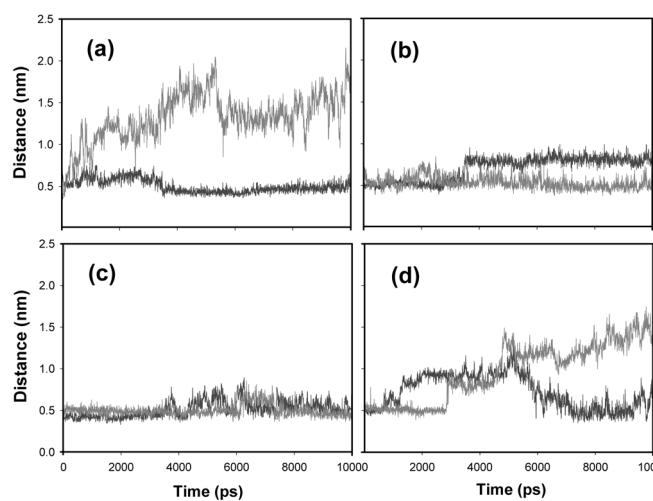


**Figure 8.** Interatomic C $\alpha$  distances between fA $\beta$  sheaf 1 and 2 (a), 2 and 3 (b), 3 and 4 (c), 4 and 5. (d). Red line indicates fA $\beta$  fibrils with myricetin and blue line indicates fA $\beta$  fibrils alone.

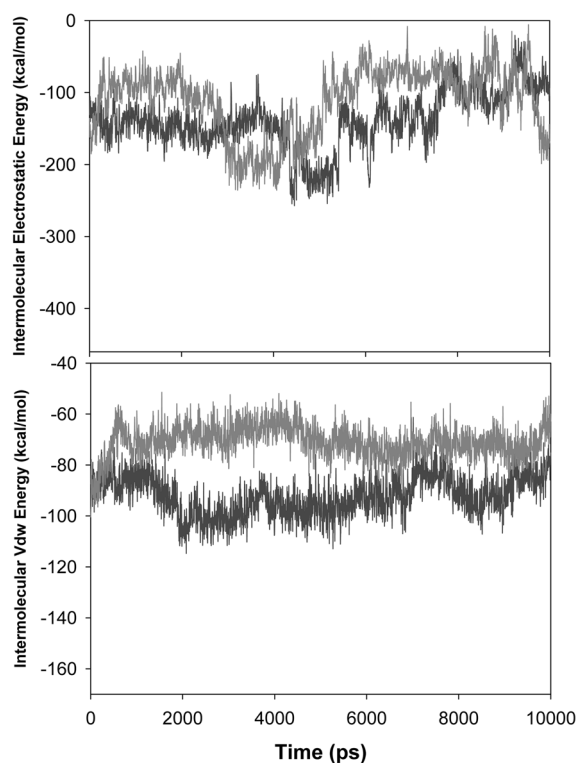


**Figure 9.** Intermolecular electrostatic (a) and vdw energy (b) between outermost fA $\beta$  sheaf. Red line indicates fA $\beta$  fibrils with myricetin and blue line indicates fA $\beta$  fibrils alone.

During MD simulations, the intermolecular electrostatic energies were controversial to each fA $\beta$  fibril with and without myricetin (Figure 9a). However, intermolecular vdw energies were discriminated between the fA $\beta$  fibrils (Figure 9b). The vdw energy of fA $\beta$  fibrils was lowered than the case of fA $\beta$  fibrils with myricetin system during the simulation times. Intermolecular vdw energy was  $-91.2$  kcal/mol for the fA $\beta$  fibrils without myricetin and  $-71.3$  kcal/mol for the fA $\beta$  fibrils with myricetin, respectively. That means myricetin molecule destabilize the intermolecular vdw interaction between outer part of fA $\beta$  sheaf rather than interior part of fA $\beta$  fibrils.

## Methods of Computation

**Construction of the molecular models and protocol of MC docking simulations.** The starting configuration of each A $\beta$  and fA $\beta$  for MC simulations was obtained from the Protein Data Bank (PDB). The PDB ID's for A $\beta$  and fA $\beta$  were 1zoq and 2beg, respectively. To obtain representative conformations of the 3D coordinate ensemble, the Discovery Studio/Builder module (version 1.7, Accelrys Software Inc.) was used as a molecular editor. The atomic coordinates and atomic partial charges of the myricetin were obtained by utilizing *ab initio* calculations with 6-311G basis set at Hartree-Fork (HF) level. All simulations were performed using a general molecular modeling program, CHARMM (version 30b1), with a parm22 all-atom force field.<sup>9</sup> The MC docking simulations were performed using the "MC" module

of CHARMM. The short-range non-bonding interactions were truncated with a 13-Å cutoff. An implicit solvent water model was used with a distance-dependent dielectric constant. The docking process was assumed to be a 1:1 interaction between each amyloid peptide and myricetin during the MC runs. The initial configuration of each amyloid and myricetin molecule was positioned arbitrarily within a neighboring distance. Trials to a new configuration were accomplished by changing each move set of a guest molecule. The MC move set for flexible docking was composed of rigid translations, rigid rotations, and rotations of freely rotatable dihedral angles of the both myricetin and amyloids. A single step consists of picking a random conformer, making a random move, minimizing the energy of a new conformer, and then checking the energy with a Metropolis criterion.<sup>10</sup> The MC-accepted structures were saved every 4000 steps for 8,000,000 trials. Multiple 10-MC trajectories were generated with different random number seed to convergence of the simulation. These MC processes produced convergent docked structures for each monomeric amyloid with myricetin.

**Multiple molecular dynamics simulations of the each myricetin/A $\beta$  and myricetin/fA $\beta$  complexes.** The starting configurations of each myricetin/A $\beta$  and myricetin/fA $\beta$  complex for the MD simulations in explicit water were taken from the MC-docked conformations<sup>11</sup> with the lowest-energy value (Figure 2). The geometries of these molecular models were fully optimized before MD runs. A TIP3P three-site rigid water model was used to solvate the complexes.<sup>12</sup> Water molecules were removed if they were closer than 2.8 Å to any heavy atoms of the complexes. In summary, each system was constructed using periodic boundary conditions with a cubic box of dimensions 50 Å  $\times$  50 Å  $\times$  50 Å, consisting of myricetin/A $\beta$  complex and 4,320 water, or myricetin/fA $\beta$  complex and 4,293 water molecules. The system was minimized by 2,000 steps of conjugate gradient, followed by Adopted Basis Newton-Raphson until the root-mean-square gradient was less than 0.001 kcal/mol. The MD simulations were performed using the CHARMM 30b1 program in the isothermal-isobaric ensemble at 300 K ( $P = 1$  bar,  $T = 300$  K). The particle mesh Ewald summation method<sup>13</sup> was used to treat the long-range electrostatic interactions.<sup>14</sup> The bond lengths of all molecules were constrained with the SHAKE algorithm.<sup>15</sup> The time step was 2.0 fs, and the non-bonded pair list was updated every 25 steps. The short-range non-bonded interactions were truncated with a 13-Å cutoff. The temperature and pressure of the system were regulated using the Langevin piston method in conjunction with Hoover's thermostat.<sup>16</sup> The system was gradually heated to each targeted temperature for 50 ps and equilibrated at this temperature. The production MD trajectory with one snapshot per 2 ps was collected for 5,000 ps. Total six-independent MD simulations were performed with different random number seed to cover wide conformational sampling. For the simulation of whole fibrils with

myricetin, molecular model was constructed with the cubic box of dimensions 70 Å  $\times$  70 Å  $\times$  70 Å, consisting of four myricetins, five-fA $\beta$  fibril, and 10,216 water molecules. The MD simulations were carried out over the course of 10-ns to observe destabilization of fA $\beta$  fibril by myricetin.

## Conclusions

Comparison of the dynamics of myricetin/A $\beta$  and myricetin/fA $\beta$  complex during molecular simulations demonstrate that myricetin disturb upon Alzheimer's  $\beta$ -amyloid fibrillogenesis by preferential binding into the hydrophobic patch of fA $\beta$ . Multiple MD simulations of myricetin/A $\beta$  and myricetin/fA $\beta$  provided the important theoretical insight into the experimentally determined anti-amyloidogenic effect of flavonoid compound, suggesting that myricetin could bind to fibrous form of amyloid peptides, thereby decreasing favorable interaction between monomeric  $\beta$ -sheets of amyloid fibrils. Based on the present study, we conclude that computational methodology can make great contribution toward anti-amyloidogenic drug design using natural flavonoid compounds.

**Acknowledgments.** This study was supported by a grant of the *e*-Science Project of KISTI (Korea Institute of Science and Technology Information) in MOST (Ministry of Science and Technology) and partly supported by a grant of the Korea Research Foundation (KRF-2006-005-J03402).

## References

1. Pepys, M. B. *Annu. Rev. Med.* **2006**, *57*, 223.
2. Selkoe, D. J. *Nature* **2003**, *426*, 900.
3. Sunde, M.; Serpell, L. C.; Bartlam, M. *J. Mol. Biol.* **1997**, *273*, 729.
4. Harper, J. D.; Lansbury, P. T. Jr. *Annu. Rev. Biochem.* **1997**, *66*, 385.
5. Rochet, J. C.; Lansbury, P. T. Jr. *Curr. Opin. Struct. Biol.* **2000**, *10*, 60.
6. Luhrs, T.; Ritter, C.; Adrian, M.; Riek-Loher, D.; Bohrmann, B.; Dobeli, H.; Schubert, D.; Riek, R. *Proc. Nat. Acad. Sci. USA* **2005**, *29*, 17342.
7. Ono, K.; Yoshiike, Y.; Takashima, A.; Hasegawa, K.; Naiki, H.; Yamada, M. *J. Neurochem.* **2003**, *87*, 172.
8. Hirohata, M.; Hasegawa, K.; Yasuhara, S. T.; Ohashi, Y.; Ookoshi, T.; Ono, K.; Yamada, M.; Naiki, H. *Biochemistry* **2007**, *46*, 1888.
9. Brooks, B. R.; Bruccoleri, R. E.; Olafson, B. D.; States, D. J.; Swaminathan, S.; Karplus, M. *J. Comput. Chem.* **1983**, *4*, 187.
10. Metropolis, N.; Rosenbluth, A. W.; Rosenbluth, M. N.; Teller, A. H.; Teller, E. *J. Chem. Phys.* **1953**, *21*, 1087.
11. Choi, Y.; Park, S.; Jeong, K.; Jung, S. *Bull. Korean Chem. Soc.* **2007**, *28*, 1811.
12. Jorgensen, W. L. *J. Chem. Phys.* **1983**, *79*, 926.
13. Darden, T.; York, D.; Pedersen, L. *J. Chem. Phys.* **1993**, *98*, 10089.
14. Lee, S. H. *Bull. Korean Chem. Soc.* **2006**, *27*, 1154.
15. Ryckaert, J. P.; Ciccoliti, G.; Berendsen, H. J. C. *J. Comput. Phys.* **1977**, *23*, 327.
16. Feller, S. E.; Zhang, Y.; Pastor, R. W.; Brooks, B. R. *J. Chem. Phys.* **1995**, *103*, 4613.